

AperTO - Archivio Istituzionale Open Access dell'Università di Torino

**The five twin laws of gypsum (CaSO<sub>4</sub>\*2H<sub>2</sub>O). A theoretical comparison of the interfaces of the penetration twins**

**This is the author's manuscript**

*Original Citation:*

*Availability:*

This version is available <http://hdl.handle.net/2318/106784> since 2016-07-21T10:35:37Z

*Published version:*

DOI:10.1021/cg300227j

*Terms of use:*

Open Access

Anyone can freely access the full text of works made available as "Open Access". Works made available under a Creative Commons license can be used according to the terms and conditions of said license. Use of all other works requires consent of the right holder (author or publisher) if not exempted from copyright protection by the applicable law.

(Article begins on next page)

This is the author's final version of the contribution published as:

RUBBO M.; BRUNO M.; MASSARO F. R.; AQUILANO D.. The five twin laws of gypsum ( $\text{CaSO}_4 \cdot 2\text{H}_2\text{O}$ ). A theoretical comparison of the interfaces of the penetration twins. *CRYSTAL GROWTH & DESIGN*. 12 pp: 3018-3024.

DOI: 10.1021/cg300227j

The publisher's version is available at:

<http://pubs.acs.org/doi/abs/10.1021/cg300227j>

When citing, please refer to the published version.

Link to this full text:

<http://hdl.handle.net/2318/106784>

# The Five Twin Laws of Gypsum ( $\text{CaSO}_4 \cdot 2\text{H}_2\text{O}$ ): A Theoretical Comparison of the Interfaces of the Penetration Twins

Marco Rubbo,\* Marco Bruno, Francesco Roberto Massaro and Dino Aquilano

Dipartimento di Scienze della Terra, Università degli Studi di Torino, via V. Caluso 35, I-10125 Torino, Italy

\*Corresponding Author

E-mail: [marco.rubbo@unito.it](mailto:marco.rubbo@unito.it)

Ph: +39 011 670 5127

Fax: +39 011 670 5128

## ABSTRACT

Having assumed the flat  $\{010\}$  form as the original composition plane (OCP), the interfaces of the 100,  $\bar{1}01$ ,  $\bar{2}01$ , 001 and 101 penetration twins of gypsum crystal are theoretically examined and their relaxed structures are illustrated. The related twin energies ( $\gamma_{PT}$ ) are 357, 64, 2171, 2124 and 10844 erg  $\text{cm}^{-2}$ , respectively. The observed experimental growth shape is interpreted, for each twin law, with the aid of the theoretical one. For each twin law, a comparison is made, between the  $\gamma_{PT}$  values obtained from contact and penetration interfaces, and a global evaluation is done on their occurrence probability. Finally, for the penetration twins, a correlation is proposed among the area of the 2D common cell at the twin interface, the obliquity of the cell, the twin energy and the supersaturation domain of the mother phase in which the twin can occur.

## 1. Introduction

Five geometrical laws describe gypsum twins.<sup>1</sup> The first attempt of relating the growth morphology to these laws is due to Simon<sup>2</sup> who proposed a thorough analysis on the structure of the original composition planes (OCP) and rows (OCR) of the different twins, starting from a theoretical determination of the stability of the crystal surfaces based on the use of the Hartman-Perdok method.<sup>3</sup> Recently, we presented a systematic study on the theoretical equilibrium and growth morphology of gypsum<sup>4,5</sup> and, in particular, determined and compared the structure of the expected interfaces of the contact twins as well as the twin energies involved in the generation of the contact interfaces.<sup>6,7</sup> Accordingly, the five contact twins were grouped in three classes, following the character of the OCP and the magnitude of the interface energy ( $\gamma_{PT}$ ) between parent (P) and twinned (T) individuals:

- i) the 100 law is related to the stepped (S)  $\{100\}$  form which is part of the athermal equilibrium shape (ES) of the crystal. The interface energy of this contact twin ( $\gamma_{PT}^{100} = 13.6 \text{ erg cm}^{-2}$ ) is so low that the  $\{100\}$  surfaces are the only ones available for the 2D-nucleation of both normally and twinned oriented nuclei.
- ii) the 001 and the  $10\bar{1}$  laws are also associated to S forms, but their  $\gamma_{PT}$  values are one order of magnitude higher than that of the 100 law (145 and 255  $\text{erg cm}^{-2}$ , respectively). The large value of the ratios ( $\gamma_{PT}^{001}/\gamma_{PT}^{100}$ ) and ( $\gamma_{PT}^{\bar{1}01}/\gamma_{PT}^{100}$ ) affects the predicted nucleation frequency of the contact 001 and  $10\bar{1}$  laws in respect to that of the 100 one and accounts for the experiments by Kern and Rehn<sup>8</sup> who reported that the 001 and the  $10\bar{1}$  contact twins were never observed in growth from pure aqueous solution, while the occurrence frequency of the  $10\bar{1}$  penetration twins is largely higher than that of both contact and penetration 100 twins.
- iii) the  $\bar{2}01$  and 101 laws are related to the kinked (K)  $\{\bar{2}01\}$  and  $\{101\}$  forms. Their very large  $\gamma_{PT}$  values, 826 and 848  $\text{erg cm}^{-2}$  respectively, account for the structural instability of these forms that do not have surface sites for the nucleation of 2D islands or 1D steps either in normal or twinned position.

In this work we extend our study to the penetration twins.

Some preliminary remarks are needed about the choice of the surfaces on which the penetration twins could start. Due to the point group symmetry (2/m) of gypsum, it is fairly unsurprising that all the five twins laws correspond to  $h0l$  twin planes: as a matter of fact, the peculiar arrangement of the  $\text{SO}_4^{2-}$  tetrahedra does not allow pseudo-symmetry planes of the type  $0kl$ ,  $hk0$  or  $hkl$ .

Nevertheless, none of the composition faces of the contact twins are F and the formation of twinned nucleus on the S or K  $\{h0l\}$  forms (contact twins) occurs at high supersaturation and can be 1D, excepting the peculiar case of the 100 twin law.<sup>6</sup>

As gypsum penetration twins are abundant, a 2D twinned nucleus most likely forms on a F face of the equilibrium and/or growth morphology of gypsum such as  $\{010\}$ ,  $\{120\}$ ,  $\{011\}$  and  $\{\bar{1}11\}$ .<sup>2,4</sup>

In our opinion, the pinacoid  $\{010\}$  seems to be the best candidate as OCP, owing to its surface profile, which is not only the most stable one, but is also that exposing the highest density of structural water molecules to the mother phase.<sup>4</sup> This peculiarity favours the “flexibility” of the  $\{010\}$  interface to accommodate twinned nuclei on it, since any new nucleus (either normal or twinned) has to share with the  $\{010\}$  pre-existing substrate of relatively mobile double layer of water molecules. The analysis of this kind of “soft” interface will be a main subject of this paper;

moreover we propose some general considerations based on growth mechanisms to rationalize the morphology of the five twins. At this end we will:

- i) assess the coincidence lattices between P and T individuals at the common  $\{010\}$  interface, assumed as OCP;
- ii) calculate the twin energies and evaluate the probability of observation of the different kind of penetration twins and associated twin laws;
- iii) compare the energy of contact and penetration twins.

As in preceding papers,<sup>4-7</sup> we adopted the reference frame chosen by De Jong and Bouman,<sup>9</sup> Cole and Lancucki<sup>10</sup> and Hejinen and Hartman.<sup>11</sup>

## 2. Growth morphology, composition plane and 2D-coincidence lattices of the five penetration twins

The five geometrical twin laws of gypsum originate peculiar inter-penetrated growth morphologies when the OCP coincides with the faces of the pinacoid  $\{010\}$ . We calculated the different shapes of the penetration twins using the rich statistical data on the growth twins described in literature and assuming a constant ratio among the advancement rates ( $R_{hkl}$ ) of the three slowest growing crystal forms, i.e.:  $R_{\{010\}} \ll R_{\{120\}} < R_{\{\bar{1}11\}}$ . The drawings of the 010 platy penetration twins are presented in Figs. 1-5. For the sake of clarity, the relevant directions of each bi-crystal are indicated: the  $[\bar{1}01]$  direction, i.e. the zone axis of the  $\{\bar{1}11\}$  and  $\{010\}$  forms, and the  $[001]$  direction, the zone axis of the  $\{120\}$  and  $\{010\}$  forms. In column b (Figs. 1-5) the common meshes of the 2D coincidence lattices (between P and T crystals) on the 010 OCP along with their obliquity are described; the reference frames ( $X_{P,T}, Z_{P,T}$ ) of each twin are also outlined.

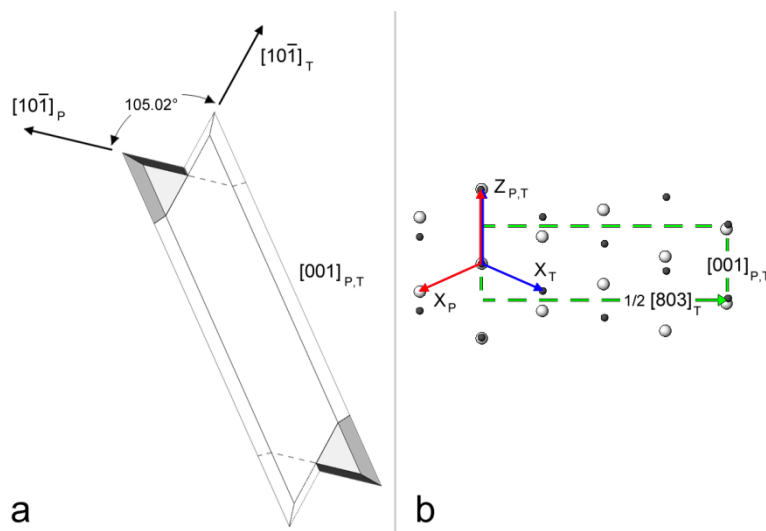


**Figure 1.** (a) Simulation of the 100 penetration twin projected on the 010 original composition plane (OCP). (b) One half of the 2D coincidence lattice shared by P and T individuals on the OCP surface.

The 100 penetration twin commonly looks  $[001]$  elongated, as shown in Fig. 1a, the P and T individuals overlapping each other on their common  $\{010\}$  surfaces. A “swallow tail” is formed between the twinned  $[10\bar{1}]$  edges and is characterized by a re-entrant obtuse angle of  $105.02^\circ$ . The interface that generates when a twinned T nucleus (either 2D or 3D) forms on a pre-existing  $\{010\}$  surface of a P individual, is defined by a centred rectangular mesh  $[001] \times [803]$ , where the  $[001]_{P,T}$  direction corresponds to the  $A_2$  axis operation lying in the 100 twin plane. The area of the mesh is quite large ( $260.16 \text{ \AA}^2$ ), while its obliquity is very low ( $0.60^\circ$ ) as it can be appreciated in Fig. 1b.

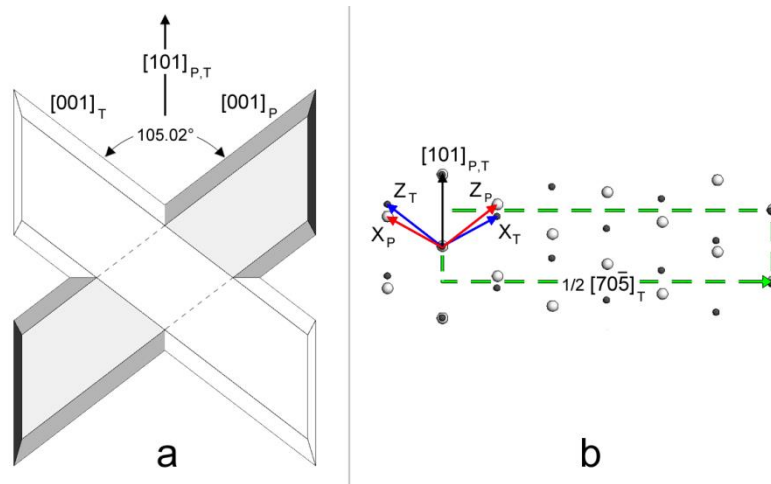


**Figure 2.** (a) Simulation of the  $10\bar{1}$  penetration twin projected on the 010 OCP. (b) One half of the quasi-perfect rectangular 2D coincidence lattice shared by P and T individuals on the OCP surface.

As outlined when comparing the interfaces of the contact twins of gypsum,<sup>7</sup> the similarity between 100 and  $10\bar{1}$  twin laws is not limited to the contact twins but extends to the penetration ones. Actually, one could remark that the growth shapes shown in Figs. 1a and 2a are rather different, due to the acute angle formed by the  $[001]_{P,T}$  edges. Nevertheless, this acute angle can be filled during growth owing to the re-entrant angle effect occurring at the intersection of the  $\{120\}$  forms of both individuals of the twin. Consequently, the overall shape of 100 and  $10\bar{1}$  penetration twins should be hardly distinguishable, especially if one takes into account that the obtuse angle between the  $[001]_{P,T}$  directions (Fig. 2a) is rigorously the same as that illustrated in Fig. 1a. The morphological difference between 100 and  $10\bar{1}$  penetration twins should then reduce to the higher shape elongation of the 100 twins, because its obtuse angle is formed by the  $[10\bar{1}]$  edges advancing faster than the  $[001]$  ones. Summing up, the only way to correctly identify these two penetration twins,

commonly called 100 – “swallow tail” and  $\bar{1}01$  – “Montmartre twin”, consists in comparing their optical extinction under crossed polarizers, as we already suggested in a preceding paper.<sup>7</sup>

Considering the interface of the  $\bar{1}01$  penetration twin, we see that the centred rectangular mesh drawn in Fig. 2b shows that the  $A_2$  axis operation lying in the  $\bar{1}01$  twin plane coincides with the direction  $[101]_{P,T}$ . The mesh area is  $[101] \times [\bar{7}05] = 390.10 \text{ \AA}^2$ , i.e. 50% larger than that of the 100 penetration twin, whereas the obliquity reaches, in this case, the lowest value of the five twin laws ( $0.089^\circ$ ).

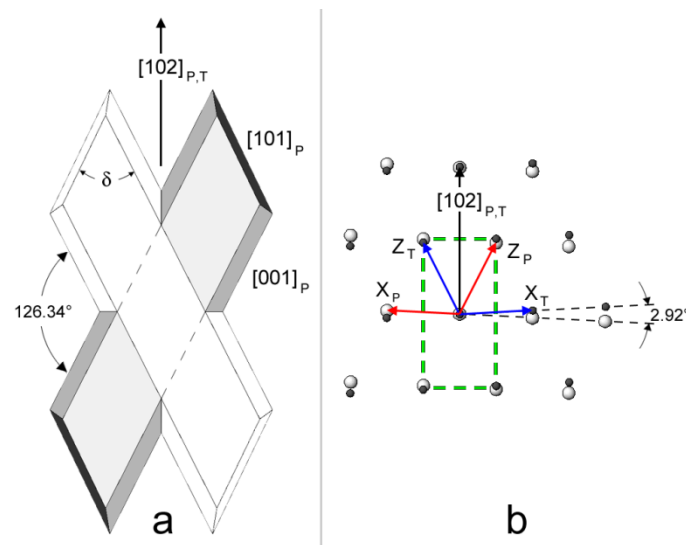


**Figure 3.** (a) Simulation of the  $\bar{1}01$  penetration twin projected on the 010 OCP. (b) The 2D coincidence lattice shared by P and T individuals on the OCP surface.

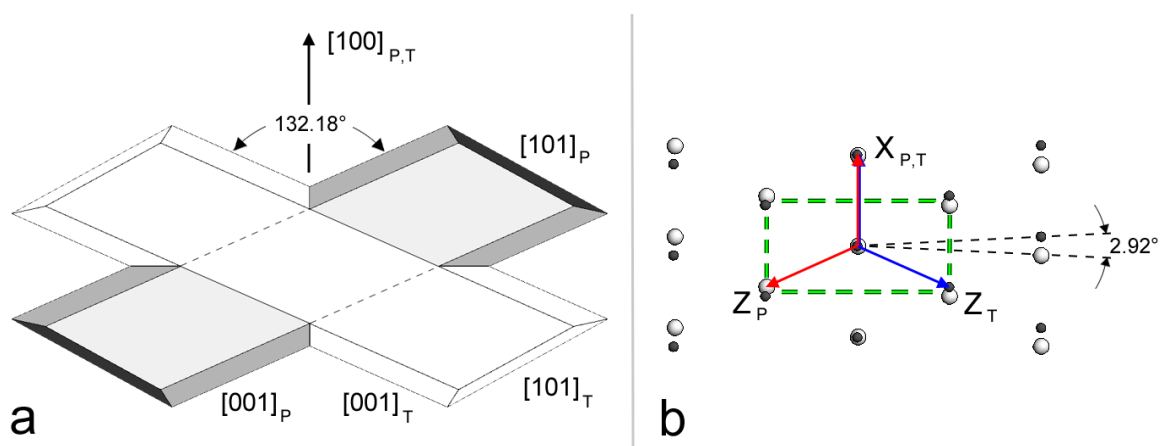


**Figure 4.** (a) Simulation of the 001 penetration twin projected on the 010 OCP. (b) The 2D coincidence lattice shared by P and T individuals on the OCP surface.

The  $\bar{2}01$  and  $001$  penetration twins have to be treated together, owing to the striking similarity of both their growth morphology and lattice interfaces on the  $010$  OCP. As a matter of fact, the only evident difference between Figs. 3a and Fig. 4a lies in the obtuse angle which assumes the value of  $126.34^\circ$ , in the  $\bar{2}01$  law, while increases to  $132.18^\circ$  in the  $001$  penetration twin. The small difference close to  $6^\circ$  is the unique morphological criterion to differentiate these two penetration twins. This cannot be neglected considering that the growth kinetics in the obtuse angle is ruled, in both twins, by the same crystal forms, i.e. the  $\{120\}$  prisms.

A special consideration is deserved to the interfaces on  $010$ , the original composition plane. Figs. 3b and 4b clearly show that both penetration twins have the same small coincidence mesh  $[102] \times [100] = 65.04 \text{ \AA}^2$ . The  $A_2$  twin axis coincides with the  $[102]_{P,T}$  row in the  $\bar{2}01$  twin, while the  $[100]_{P,T}$  row plays the role of the twin axis in the  $001$  twin. At variance with the  $100$  and  $\bar{1}01$  penetration twins where the meshes of their 2D coincidence lattices are large but the mesh obliquities are practically negligible, the  $\bar{2}01$  and  $001$  penetration twins show very small common meshes but their coincidence is characterized by a relevant obliquity close to  $3^\circ$ .

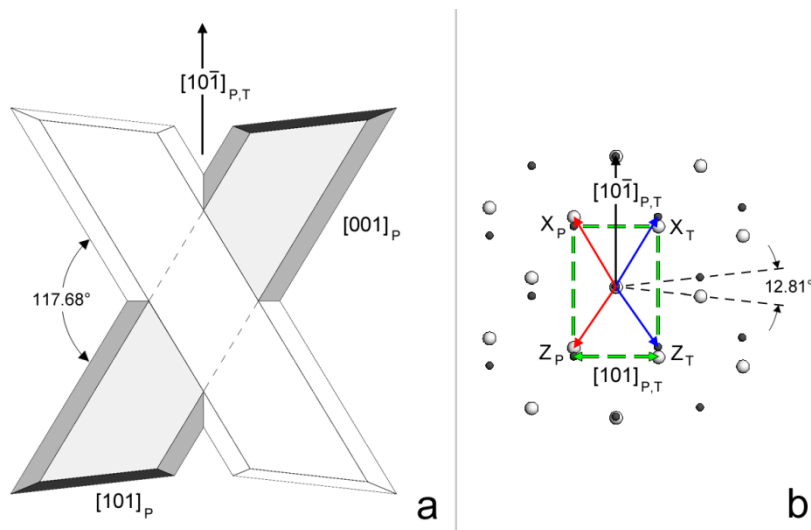


**Figure 5.** (a) Simulation of the  $101$  penetration twin projected on the  $010$  (OCP). (b) The 2D coincidence lattice shared by P and T individuals on the OCP surface. The pseudo-rectangular lattice mesh is  $[10\bar{1}] \times [101] = 65.097 \text{ \AA}^2$  and the angular misfit reaches  $12.81^\circ$ .

Finally, the morphology of the X-shaped  $101$  penetration twins (Fig. 5a) is likely to be mistaken for that of the  $\bar{1}01$  or  $100$  twins, especially when the acute angle formed by the  $[001]$  edges is filled up during growth. But, looking at this  $010$  penetration interface, it leaps off that the coincidence lattice is the worst among the five twinned interfaces, its obliquity reaching a value close to  $13^\circ$ .



### 3. The calculation method of the twin energy on the 010 OCP and the relaxed penetration interfaces of the five twins

In the following we describe the method we used to generate the penetration twins and then we characterize them. A 2D-slab model was adopted:

- (i) at first, a crystal slab (slab P) of a given thickness was made by cutting the optimized bulk structure parallel to the composition plane 010; the cut corresponds to the water-terminated {010} surface profile.
- (ii) Then, a second slab (slab T) was made by applying the appropriate twin law to the atomic coordinates of the slab P.

In order to avoid generating a fictitious stress due to the obliquity of the 2D lattices of the P and T slabs (Figs. 1-5), a 2D rectangular cell common to both the slabs must be considered; the values of the 2D lattice parameters used for the calculation are reported in Table 1.

To set an initial configuration of the interface between the two slabs, the P and T slabs are moved one relatively to the other; ions and molecules can also be displaced to avoid any evident repulsions. In this way several initial configurations can be tested. The energy of the bi-crystal (slab P + slab T) is then minimized under the constraints of constant volume and two dimensional periodic boundary conditions.

Twin law	2D lattice parameters (Å)	
100	$ [301]  = 15.3779$	$ [001]  = 6.2592$
$10\bar{1}$	$ [30\bar{2}]  = 24.5921$	$ [101]  = 6.5233$
001	$ [100]  = 5.5879$	$ [102]  = 11.4837$
$\bar{2}01$	$ [100]  = 5.5801$	$ [102]  = 11.4995$
101	$ [10\bar{1}]  = 9.9121$	$ [101]  = 6.4738$

**Table 1.** The 2D lattice parameters of the rectangular cells of the twinned slabs (slab P + slab T) used for the geometry optimizations at constant volume.

We used the program GDIS<sup>12</sup> to build the slabs and the program GULP<sup>13</sup> for the energy calculations. As in our previous works on contact twins of gypsum,<sup>6,7</sup> we used the force field proposed by Adam.<sup>14</sup> Geometry optimization is considered converged when the gradient tolerance and the function tolerance (*gtol* and *ftol* adimensional parameters in GULP) are smaller than  $10^{-5}$  and  $10^{-6}$ , respectively.

The energy of the interface is the difference of energy, per unit surface area ( $S$ ), between the twinned crystal ( $E_{PT}$ ) and the not twinned one ( $E_{untwinned}$ ) comprising the same number of atoms and exhibiting the same outmost layers. Then, the twin energy is an interfacial energy ( $\gamma_{PT}$ ):

$$\gamma_{PT} = \frac{E_{PT} - E_{untwinned}}{S}$$

In Fig. 6 the  $[10\bar{1}]$  view of the interface of the  $10\bar{1}$  penetration twin is illustrated, as obtained after relaxation. The vector  $[10\bar{1}]$  which is parallel to the twin axis, along with its pseudo-normal vector  $[30\bar{2}]$ , identify the 2D coincidence mesh that is shared by P and T individuals on the OCP. The pseudo-normal vector  $[30\bar{2}]$  (having an angular misfit of  $1.19^\circ$ ) was chosen, instead of the normal vector  $[70\bar{5}]$  (which shows a negligible angular misfit of  $0.089^\circ$ ), in order to improve the convergence of the twin energy calculation owing to the finiteness of the crystal slab thickness. The  $10\bar{1}$  interface has been chosen as the best example of the five 010 penetration interfaces, while the remaining ones are at the reader's disposal in the Supporting Information.

Looking at the interface layer, one can see that the water molecules are disordered and the sulfate tetrahedra undergo a sensible rotation around the  $[010]$  axis. This is the relaxation mode adapting the structures of the  $d_{020}$  layers whose regular stacking is broken at the interface between T and P crystals.

What is really surprising is that a nearly perfect structural continuity obtains, across the interface, after its relaxation. As a matter of fact, either Calcium or Sulfate ions are aligned along uninterrupted directions when passing from P to T individual, as results from Fig. 6 where the  $[010]$  and  $[7.12.\bar{5}]$  vectors are clearly visible. Although the alignment of the growth units occurs along crystallographic directions in all the penetration twins, none of these directions is a PBC of the crystal, at variance with what occurs in the case of contact twins<sup>7</sup>. This means that the birth and spread of a twinned nucleus on the  $\{010\}$  surfaces is not controlled by strong bonds across the twinned interface but the growth units forming the 2D nucleus "choose" the suitable 010 surface sites and relax in order to optimize their lateral interactions. In a schematic way we could say that the relaxation in the interface region optimizes the slice energy in the case of penetration twins, and the attachment energy in case of contact twins.

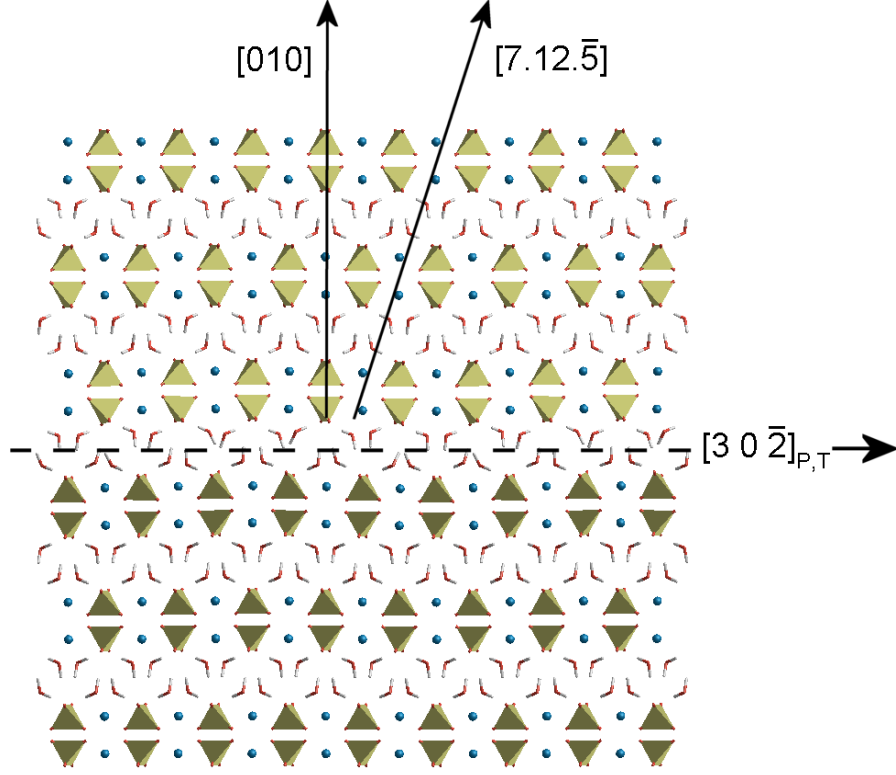


**Figure 6.** The relaxed interface of the  $10\bar{1}$  penetration twin, viewed along the twin axis  $[101]$ . The vector  $[101]$ , along with its pseudo-normal vector  $[30\bar{2}]$ , identify the 2D coincidence mesh that is shared by P and T individuals on the OCP and that was chosen for calculation.

#### 4. The twin energies. A comparison between the contact and penetration twins and the inferred distribution of twins' type

In Table 2 the calculated twin energies ( $\gamma_{PT}$ ) are summarized, for both contact<sup>7</sup> and penetration twins. The character of the surfaces on which the twinning occurs is also recollected.

Twin law	Character of the OCP (contact)	$\gamma_{PT}$		Obliquity ( $^\circ$ ) of the penetration 2D common cell	
		CONTACT (erg cm <sup>-2</sup> )	Character of the OCP (penetration)		PENETRATION (erg cm <sup>-2</sup> )
100	S	14	010 - F	357	0.6
$10\bar{1}$	S	255	010 - F	64	0.089
001	S	145	010 - F	2124	2.92
$\bar{2}01$	K	826	010 - F	2171	2.92
101	K	848	010 - F	10844	12.81

**Table 2.** A comparison between the calculated energy ( $\gamma_{PT}$ ) of twins described by the five different twin laws. For each law, we report the  $\gamma_{PT}$  the values of both contact and penetration twins.

Remembering that lower the twin energy, higher the occurrence probability of a twin, according to the  $\gamma_{PT}$  values in Table 2, three different “theoretical situations” can be distinguished:

- (i) the most frequently occurring laws should be: 100 and  $10\bar{1}$ . The privileged contact twin is 100, while  $10\bar{1}$  is the dominant penetration twin;
- (ii) the scarcely occurring laws should be:  $\bar{2}01$  and 101, owing to the high values of the twin energy, in both cases contact or penetration;
- (iii) the frequency of occurrence of the 001 law falls in between the preceding two as the occurrence of the contact twin should be even higher than that of  $10\bar{1}$  contact, while the 001 penetration twin should never be observed, due to the high twin energy.

In the following, other considerations are made to explain the observed occurrence frequency of gypsum twins.

#### 4.1. The factors favoring the occurrence of the $10\bar{1}$ penetration twins

The F character of the {010} form, which dominates both the theoretical equilibrium (ES) and growth (GS) shape of gypsum, along with the moderate value ( $\gamma_{PT}^{010} = 64 \text{ erg cm}^{-2}$ ) of the  $10\bar{1}$  twin energy, could explain why the  $10\bar{1}$  twin law only appears, in laboratory grown crystals, as a penetration twin nucleating on the original 010 composition plane.<sup>8</sup> In fact, the  $\gamma_{PT}^{010}$  value represents a moderate increase (+ 14.8%) in respect to the surface energy value ( $\gamma_{010} = 432 \text{ erg cm}^{-2}$ ) of the fresh surfaces on which a regular (non twinned) nucleation can occur.<sup>4</sup>

#### 4.2. The growth shapes of 100 contact and penetration twins

The {100} form is a stepped one. Nevertheless, it belongs to the athermal equilibrium shape (ES) of the crystal, due to the moderate value of its surface energy ( $\gamma_{100} = 678 \text{ erg cm}^{-2}$ ).<sup>4</sup> It can be also demonstrated that also at room temperature and in the presence of water adsorption this form enters the ES of the crystal. This means that, at the early stages of the crystallization, 100 twinned embryos could nucleate on the {100} form. Its surface can be the original composition plane, the lowest twin energy ( $\gamma_{PT}^{100} = 13.6 \text{ erg cm}^{-2}$  represents only 2% increase of  $\gamma_{100}$ ) accounting for the ease of formation of 100 contact twins in nature and laboratory.

Both observation and theoretical arguments prove that the {100} form cannot appear on the growth morphology of single gypsum crystals. Let's consider a 3D critical nucleus of a single gypsum crystal containing the {100} form, as it ensues from its equilibrium shape. Once the 3D embryo

becomes supercritical, the normal growth rates ( $R_{hkl}$ ) of the different  $\{hkl\}$  forms, initially composing the ES, determine the onset of the growth morphology.

Fig. 7a schematizes the evolution of the crystal viewed along its [001] axis. The inner cross section represents a hypothetical crystal shape limited by the forms  $\{010\}$ ,  $\{120\}$  and  $\{100\}$ . The successive sections are drawn having considered that, from observation in pure aqueous medium and theory:<sup>2,9</sup>  $R_{\{100\}} \gg R_{\{120\}} > R_{\{010\}}$ . Hence, both for kinetic and geometrical reasons, the  $\{100\}$  form cannot appear on the growth form, in agreement with the observation of natural and laboratory grown single crystals.

The 100 interface becomes stable and is preserved during growth only if a 100 contact twinning occurs. In fact, as it was just mentioned, either 2D or 3D twinned embryos can form in the early stage of the nucleation on the  $\{100\}$  form of a single crystal, owing to the quasi negligible  $\gamma_{PT}^{100}$  value; successively, during the growth of the bi-crystal, the twinned interface behaves as proposed in Fig. 7b, becoming the only surface of separation of the growth twin.

#### **4.2.1. How the growth shape of the 100 contact twins develops**

It is not surprising that the  $\{010\}$  surfaces of the two individuals composing the contact 100 twins could not be distinguished in the growth morphology of the bicrystal, if not by means of their different optical orientation. In fact, in the reentrant angles formed by the four  $\{120\}$  surfaces determining the twinned interface, the advancement rate must be higher than that of the adjacent  $\{010\}$  surfaces (see Fig. 7b) for two cooperating effects:

- (i) first,  $R_{\{120\}} > R_{\{010\}}$ , as mentioned above;
- (ii) second, the reentrant angle enhances the advancement rate of the faces forming it, because the 2D nucleation is favored for geometrical reasons,<sup>15</sup> and because in the reentrant angles the dislocation density may increase at the twin interface.

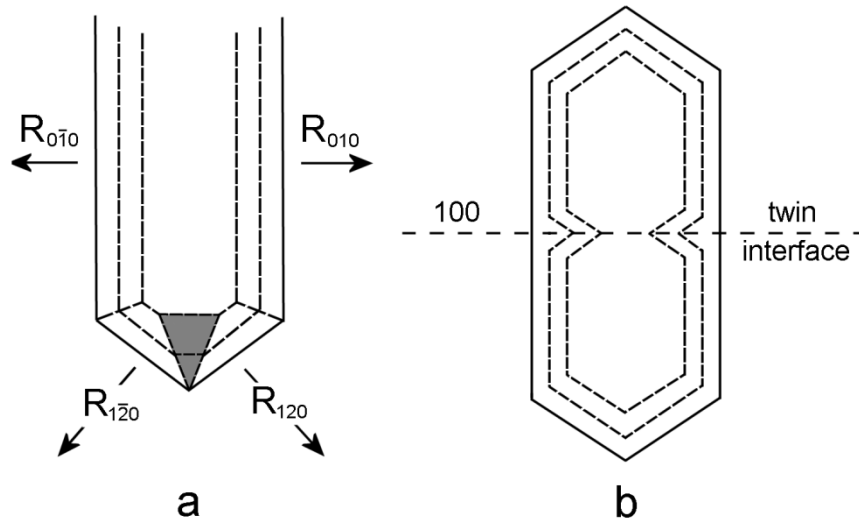


**Figure 7.** (a) Schematic drawing of gypsum crystal viewed along the [001] axis. Three successive stages of growth are simulated. Having assumed the following relation among the growth rates:  $R_{\{100\}} \gg R_{\{120\}} > R_{\{010\}}$ , the  $\{100\}$  form is doomed to escape from the growth shape of the crystal. (b) 100 contact twin, drawn in the same orientation as in (a): owing to the relation  $R_{\{120\}} > R_{\{010\}}$ , the reentrant angle vanishes during growth and, simultaneously, the 100 interface broadens.

#### 4.2.2. The growth shapes of 100 contact and penetration twins cannot be distinguished at first sight

A last consideration should be made on the occurrence frequency of the 100 twin law in laboratory grown crystals. Kern and Rehn<sup>8</sup> observed that "... the 100 penetration twins are more frequently occurring than the 100 contact twins, for every supersaturation value of the mother phase". This apparently does not agree with the hierarchy of the twin energies (13.6 versus 357 erg cm<sup>-2</sup>) for the contact and penetration mechanism, respectively. However, we remember that contact and penetration twinning cannot be always discriminated, excepted at the early stage of the twin nucleation.

Let's consider, as an example, a penetration 100 twin with the twinned nucleus initially formed on a (010) original composition face. During growth, the twinned nucleus spreads on the (010) surface and progressively overwhelms its substrate; at the end of the growth process the two individuals have encompassed each other and, finally, a penetration twin can be observed. Consequently, a bi-crystal formed by a penetration mechanism will never transform in a contact twin.

On the contrary, a twin, initially formed by contact, can evolve by two paths:

- 1) the 100 OCP separates the P and T individuals nucleated at the same time (3D twinned nuclei) having the same volume. In this case, neither of the two individuals will invade the space competing to the other one and the final twin shape will appear rigorously by contact.

- 2) the 100 OCP separates the P and T individuals, nucleated at different time, having different volume. In this case, the elder individual can likely encompass the younger one and, consequently, an early contact twin inevitably transforms in a penetration one.

This suggests that the experimental occurrence frequency of the early contact twins (for a given twin law) could be easily underestimated with respect to that observed for the early penetration twins that, in turn, could be overestimated.

#### 4.3. Both $\{10\bar{1}\}$ and $\{001\}$ forms are stepped and do not enter the athermal ES of the crystal

At 0 K the  $\{10\bar{1}\}$  form is not on the Wulff plot; at room temperature it could compose the equilibrium habit of gypsum if its energy decreased by about 17% by the thermal contribution ( $-T \times S$ ). From literature data<sup>16</sup> one can estimate that this reduction is too high, so we should conclude that the  $\{10\bar{1}\}$  form hardly belongs to the crystal ES under natural or laboratory growth conditions. This theoretical consideration is coherent with the Kern's experiments who never observed laboratory grown  $\{10\bar{1}\}$  contact twins.

Conversely, in case of the 001 contact twin it is sufficient only a 2.4% decrease of the surface energy ( $\gamma_{001}$ ) to make the  $\{001\}$  form stable at room temperature. Contrary to the previous case, this reduction is possible. Thus, it is highly probable that the  $\{001\}$  form composes the ES in natural conditions.

#### 4.4. The very peculiar case represented by the $\{001\}$ and $\{\bar{2}01\}$ penetration twins

Recollecting the interface properties of these two penetration twins described in Section 2, and having in mind the  $\gamma_{PT}$  values of the contact mode (Table 2), it becomes easy to understand the relationships between the lattice geometry and the energy properties:

- (i) the  $\gamma_{PT}$  values of these two penetration twins are equal within the limits of the calculation errors, as we obtain 3425 and 3412 erg cm<sup>-2</sup>, respectively. Hence, the related *occurrence probability is small for both  $\{001\}$  and  $\{\bar{2}01\}$  penetration twins.*
- (ii) an opposite situation is obtained for the contact twins, where the  $\gamma_{PT}$  values are sharply different, being  $\gamma_{PT}^{001} = 145$  and  $\gamma_{PT}^{\bar{2}01} = 826$  erg cm<sup>-2</sup>.

As we recently demonstrated,<sup>6</sup> this is due to the character of the  $\{001\}$  S, and  $\{\bar{2}01\}$  K, interfaces where the contact twins form. In the first case the PBC rows preserve the local symmetry while in the  $\{\bar{2}01\}$  interface layer the atoms are more free to relax in 2D uncorrelated structures quite different from the bulk.

Summing up, the comparison between the energetic and genetic characteristics of the  $\{001\}$  and  $\{\bar{2}01\}$  twin laws represents an outstanding example that *the complexity of the growth twinning cannot be reduced to the relationships between two 3D lattices mutually related by pure geometrical and structural symmetry operations*. As a matter of fact, we have just shown that two sharply different twin laws can originate either two contact twins having different occurrence probability or two penetration twins affected by the very same occurrence. This emphasizes the role of the crystal surfaces on which the “twinning reaction” starts, and sounds a note of caution in considering growth twins as 3D infinite objects built by two interpenetrating ideal lattices, as is usually done by those crystallographers caring only about the description of the relationships between lattices.

## 5. Conclusions.

The theoretical investigation on the penetration twins of gypsum allowed to integrate and partially modify our previous conclusions on the gypsum twinning.<sup>6,7</sup>

(i) At first we stress the strategic importance of determining the coincidence lattices and evaluating the twin energy involved in contact and penetration twinning mode. A complementary tool is to draw the simulated growth morphology of the twins to obtain a reasonable comparison with the observed shapes. This multistep operation allows not only to describe “quantitatively” the gypsum twins, but also to avoid as much as possible the attribution of a wrong twin law to the observed morphology. As a matter of fact we showed that:

- 1) the 100 and  $10\bar{1}$  contact twins can be easily confused from the morphological point of view, (see also the preceding paper,<sup>6</sup>) confirming an original intuition by Cody and Cody;<sup>17,18</sup>
- 2) a similar confusion can occur from the comparison of the growth shapes of either the couple 100 and  $10\bar{1}$  or the couple 001 and  $\bar{2}01$  penetration twins.

(ii) The 100 and  $10\bar{1}$  twin laws are the most important ones, even if a sharp distinction is needed about the twinning mode: the contact twin is theoretically favored for the 100 law, while the occurrence frequency of the  $10\bar{1}$  law is mainly due to the penetration mode. Furthermore, a deep analysis on the transformation from the contact to the penetration mechanisms, allows us to explain how the occurrence of the 100 contact twins could be underestimated and thus that of both 100 and  $10\bar{1}$  penetration twins overestimated. The



picture we propose agrees with Kern and Rehn results and interpretation,<sup>8</sup> but they overestimated the occurrence of both 100 and  $10\bar{1}$  penetration twins.

(iii) In the contact twins, the obliquity of the common 2D cell at the twin interface is nil, owing to the twin operation (either mirror or axis). Hence the contact twin energy,  $\gamma_{PT}$ , is ruled by other parameters:

- 1) the stepped (S) character of the  $\{100\}$ ,  $\{10\bar{1}\}$  and  $\{001\}$  forms, which lowers the  $\gamma_{PT}$  value with respect to that of the kinked (K) ones,  $\{\bar{2}01\}$  and  $\{101\}$ ;
- 2) the area of the 2D cell at the twin interface, which is roughly 50% larger for the  $\{\bar{2}01\}$  and  $\{101\}$ , in respect to the  $\{100\}$ ,  $\{10\bar{1}\}$  and  $\{001\}$  forms;
- 3) for a given value of the 2D cell area at the twin interface, a factor lowering the  $\gamma_{PT}$  value is the continuity of the periodic bond chains crossing the interface.<sup>7</sup>

(iv) In the penetration twins, at variance with the contact ones, the obliquity of the 2D interface common cell is a factor that heavily affects the value of the twin energy. It is not by chance that lower the obliquity, lower the  $\gamma_{PT}$  value of the corresponding penetration interface, as it ensues from the two last columns in Table 2.

(v) The area of the 2D common cell at the penetration interface is a parameter that must be analyzed too. A 2D embryo must fit in the large area ( $390 \text{ \AA}^2$ ) of the 2D common cell of the  $10\bar{1}$  penetration twin; as the obliquity ( $0.089^\circ$ ) is low as well as the twin energy ( $\gamma_{PT} = 64 \text{ erg cm}^{-2}$ ), such embryo can nucleate at low supersaturation. This is consistent with the experimental observations by Simon,<sup>2</sup> by Kern and Rehn<sup>8</sup> and with the wide occurrence of the  $10\bar{1}$  penetration twins in nature. On the contrary, the small areas ( $65 \text{ \AA}^2$ ) of the 2D common cells of the 001,  $20\bar{1}$  and 101 penetration twins, coupled with their high or very high obliquity ( $2.92^\circ$ ,  $2.92^\circ$  and  $12.82^\circ$ , respectively) and with their very high  $\gamma_{PT}$  values ( $2124$ ,  $2171$  and  $10844 \text{ erg cm}^{-2}$ , respectively), are compatible with small twinned embryos nucleating at higher supersaturation.

Summing up, we conclude recollecting the method followed and the results presented in three papers on gypsum twinning (ref. 6, 7 and the present one).

The calculation of the twin energy allowed us to go beyond the limits of a description of the lattice geometry of the twins, which is necessary but not sufficient to unravel the evolution path of a growth twin. The structural analysis of the surfaces on which a faulted nucleus starts growing has been the unavoidable preliminary step, in order to obtain the relaxed structure of both contact and penetration interfaces and the  $\gamma_{PT}$  values. Thanks to that, the occurrence frequency of the contact and penetration twins was estimated.

The simulated twin morphology made evident the erroneous identification, reported in literature, of the two main twin laws and the risk of confusing the  $\bar{2}01$  with the 001 penetration twins.

Nevertheless, new improvements are needed in order to understand how water and impurities may modify the calculated occurrence frequency of the twins and change their morphology.

One can reasonably assume that water adsorption cannot modify the estimated probability of occurrence of twins, owing to the different order of magnitude of the athermal twin energies in vacuum; however, we expect changes in the growth morphology due to water adsorption,<sup>19</sup> as well as to adsorption/absorption of specific additives.<sup>2</sup>

Due to the relevance of gypsum twinning in both industrial and geological fields, the adsorption of water and specific impurities on gypsum surfaces will be the subject of our future research.

**Supporting Information Available.** The optimized structure of the interfaces of the 100, 001,  $\bar{2}01$  and 101 penetration twins. This material is available free of charge via the Internet at <http://pubs.acs.org>.

## References

- [1] Follner, S.; Wolter, A.; Helming, K.; Silber, C.; Bartels, H.; Follner, H. *Cryst. Res. Technol.* **2002**, *37*, 207-218.
- [2] Simon, B. *Contribution à l'étude de la Formation des Macles de Croissance*; Thèse docteur ès-Sciences Physiques: Marseille, France, 1968.
- [3] Hartman, P. In *Crystal Growth: An Introduction*; Hartman P. Ed.; North Holland Publishing Co.; Amsterdam 1973; pp. 367-402.
- [4] Massaro, F.R.; Rubbo, M.; Aquilano, D. *Crystal Growth & Design* **2010**, *10*, 2870-2878.
- [5] Massaro, F.R.; Rubbo, M.; Aquilano, D. *Crystal Growth & Design* **2011**, *11*, 1607-1614.
- [6] Rubbo, M.; Bruno, M.; Aquilano, D. *Crystal Growth & Design* **2011**, *11*, 2351-2357.
- [7] Rubbo, M.; Bruno, M.; Massaro, F.R.; Aquilano, D. *Crystal Growth & Design* **2012**, *12*, 264-270.
- [8] Kern, R.; Rehn, B. *C.R. Acad. Sci. Paris*, **1960**, *251*, 1300-1302.
- [9] De Jong, W.F.; Bouman, J. *Z. Kristallogr.* **1938**, *100*, 275-276.
- [10] Cole, W.E.; Lancucki, C.J. *Acta Crystallogr.* **1974**, *B30*, 921-929.
- [11] Harman, P.; Hejinen, W.M.M. *J. Crystal Growth* **1983**, *63*, 261-264.
- [12] Fleming, S.; Rohl, A. *Z. Kristallogr.* **2005**, *220*, 580-584.
- [13] Gale, J. D. *Faraday Trans.* **1997**, *93*, 629-637.
- [14] Adam, C. D. J. *Solid State Chem.* **2003**, *174*, 141-151.

- [15] Boistelle, R.; Aquilano, D. *Acta Crystallogr.* **1978**, *A34*, 406-413.
- [16] Kern R., Le Lay G., Métois J. J. in *Current Topics in Materials Science*; Kaldis E. Ed.; North Holland Publishing Co.; Amsterdam 1979; pp. 135-419.
- [17] Cody, R.D.; Cody, A.M. *Cryst. Res. Technol.* **1988**, *23*, 1437-1441.
- [18] Cody, A.M.; Cody, R.D. *J. Cryst. Growth* **1991**, *113*, 508-519.
- [19] van de Voort, E.; Hartman, P. *J. Crystal Growth* **1991**, *112*, 445-450.

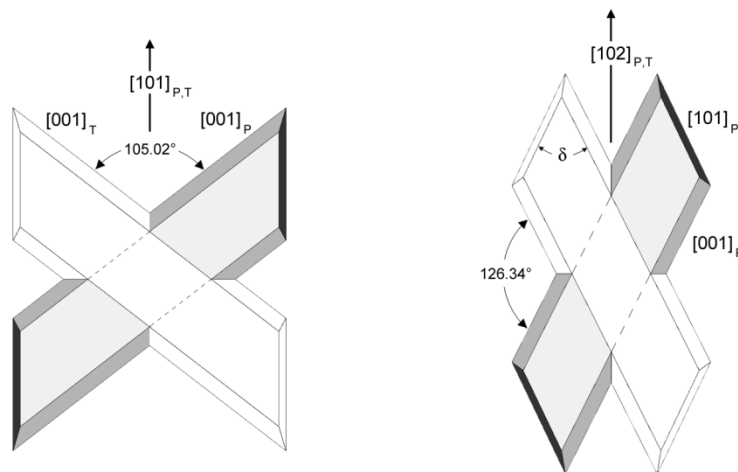
For Table of Contents Use Only

## The Five Twin Laws of Gypsum ( $\text{CaSO}_4 \cdot 2\text{H}_2\text{O}$ ): A Theoretical Comparison of the Interfaces of the Penetration Twins

RUBBO Marco, BRUNO Marco, MASSARO Francesco Roberto, AQUILANO Dino

Dipartimento di Scienze della Terra, Università degli Studi di Torino, via V. Caluso 35, I-10125  
Torino, Italy

### *The penetrations twins of gypsum*



### Synopsis

Having assumed the flat  $\{010\}$  form as the original composition plane (OCP), the interfaces of the  $100$ ,  $\bar{1}01$ ,  $\bar{2}01$ ,  $001$  and  $101$  penetration twins of gypsum crystal are theoretically examined and their morphology and relaxed structure are illustrated. The related twin energies ( $\gamma_{PT}$ ) are 357, 64, 2171, 2124 and 10844  $\text{erg cm}^{-2}$ , respectively. The observed experimental growth shape is interpreted for each twin law. A comparison is made, for each twin law, between the  $\gamma_{PT}$  values obtained from contact and penetration interfaces, and a global evaluation is done on their occurrence probability.